AGU PUBLICATIONS

Water Resources Research

RESEARCH ARTICLE
10.1002/2015WR017144

Special Section:
The 50th Anniversary of Water Resources Research

Suppressed convective rainfall by agricultural expansion in southeastern Burkina Faso

Theophile Mande[1], Natalie C. Ceperley[1], Gabriel G. Katul[2], Scott W. Tyler[3], Hamma Yacouba[4], and Marc B. Parlange[1,5]

[1]School of Architecture, Civil and Environmental Engineering, École Polytechnique Fédérale de Lausanne, Switzerland, [2]Nicholas School of the Environment, Duke University, Durham, North Carolina, USA, [3]Department of Geological Sciences and Engineering, University of Nevada, Reno, Nevada, USA, [4]International Institute for Water and Environmental Engineering (2iE), Ouagadougou, Burkina Faso, [5]Department of Civil Engineering, University of British Columbia, Vancouver, British Columbia, Canada

Key Points:
- Convective rainfall (CR) reduced by agricultural expansion in Burkina Faso
- Reductions in CR explained by reduced sensible heat (H) over agricultural sites
- Reduced H reduced crossing between ABL height and lifting condensation level

Correspondence to:
T. Mande,
theophile.mande@epfl.ch

Citation:
Mande, T., N. C. Ceperley, G. G. Katul, S. W. Tyler, H. Yacouba, and M. B. Parlange (2015), Suppressed convective rainfall by agricultural expansion in southeastern Burkina Faso, *Water Resour. Res.*, *51*, doi:10.1002/2015WR017144.

Received 21 FEB 2015
Accepted 16 JUN 2015
Accepted article online 19 JUN 2015

Abstract With the "green economy" being promoted as a path to sustainable development and food security within the African continent, the influx of agricultural land is proliferating at a rapid pace often replacing natural savannah forests. Where agriculture is primarily rainfed, the possible adverse impacts of agricultural land influx on rainfall occurrences in water-limited areas such as West Africa warrant attention. Using field observations complemented by model calculations in southeastern Burkina Faso, the main causes of a 10–30% suppressed daytime rainfall recorded over agricultural fields when referenced to natural savannah forests are examined. Measurements and model runs reveal that the crossing of the mixed layer height and lifting condensation levels, a necessary condition for cloud formation and subsequent rainfall occurrence, was 30% more frequent above the natural savannah forest. This increase in crossing statistics was primarily explained by increases in measured sensible heat flux above the savannah forest rather than differences in lifting condensation heights.

1. Introduction

Because of economic incentives and food security needs, West Africa is experiencing an unprecedented rapid expansion in agricultural land. Prototypical of this expansion is Burkina Faso, where natural savanna forests (SF) occupied some 60% of the land area in 1975. By 2000, this fraction dropped to 50% and presently is less than45%. These reductions are principally due to cropland expansion, which increased from 15% in 1975 to 23% in 2000, and are currently expanding at a rate exceeding 2% per year [*USGS*, 2013]. The croplands are primarily fed by rainfall in this region. The southern portion of Burkina Faso is still covered by large areas of SF vegetation, but there are many growing incursions of agricultural fields (AF) into this region, which may have unintended adverse impacts on convective rainfall, the focus of this work. Specifically, using a combination of measurements and model calculations, it is shown that appreciable reductions in daytime convective rainfall due to SF to AF conversion pattern cannot be discarded. In fact, much of the total daily rainfall differences between SF and AF are primarily due to daytime differences. Data were collected in the southeastern portion of Burkina Faso over 3 years at adjacent AF and SF sites using 12 advanced weather monitoring SensorScope stations and two eddy covariance (EC) flux towers. Measured variables include sensible and latent heat fluxes by EC, mean air temperature and air humidity, shortwave and net radiation as well as precipitation measured with a network of rain gages spatially distributed within AF and SF. The rainy season is characteristic of a Sudanian climate beginning in May and ending in October [*Bagayoko et al*., 2007; *Ceperley et al*., 2012; *Mande et al*., 2014]. The rainfall is short in duration, intense, and occurs mostly during daytime primarily due to convective activities [*Nicholson*, 2013].

2. Methods

The experiments were conducted around the village of Tambarga (11°26'42.79"N, 1°13'32.09"E), Kompienga city (see Figure 1), situated in southeastern Burkina Faso. The climate is semiarid and alternates between dry and wet seasons. These sites were selected because the savanna forest in the commune of Madjoari around the village of Tambarga coverssome 70% of the adjacent area. This fractional coverage

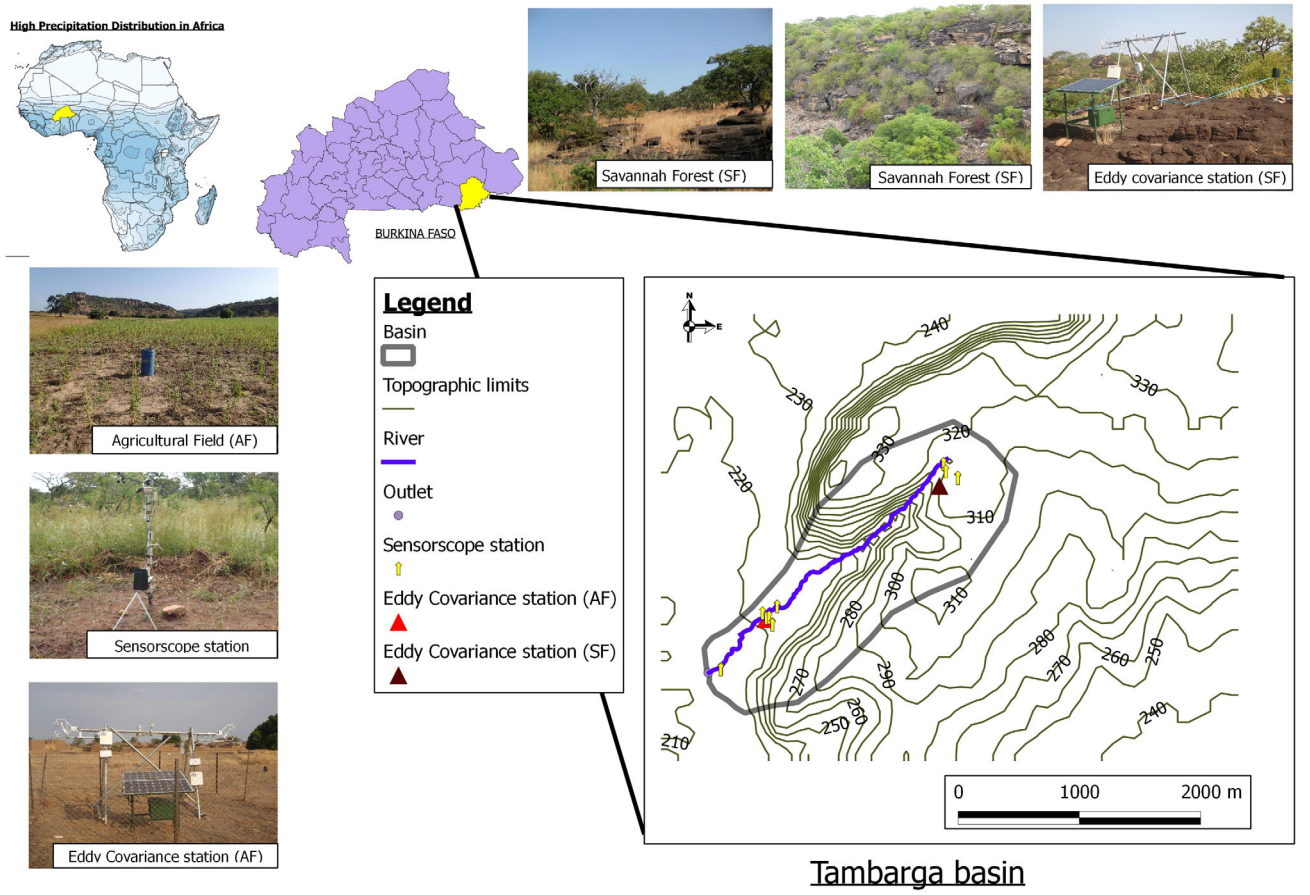

Figure 1. The top left map is rainfall distribution within the African content with lightest color indicating low rainfall (100 mm yr^{-1}) and the dark blue color indicating the most intense rainfall (> 2000 mm yr^{-1}). The location and topography of the Tambarga basin as well as the map of Burkina Faso are also shown. Photos of the Ss and EC stations along with the AF and SF land cover are presented for reference. The scale in the topo-map is in meters.

increases to some 90% if the surrounding Singou's basin is also included, as this aforementioned basin is classified as protected hunting zone since 2006. However, agricultural expansion is proliferating in this area, which is why this region was selected for the experiments here.

Two sites SF and AF, separated by more than 1500 m, were chosen for micrometeorological measurements representing how agricultural land conversion of natural savannah may be impacting local climate in the region. The SF is a mosaic of grassland, shrub woodlands, and dense large trees situated at an elevation of about 100 m above the surrounding AF. The AF is a rainfed large agroforestry field used for millet and rice plantation during the rainy season. The AF soils are loamy sand with a low permeable clay layer at a depth about 1 m while the SF soils are shallower and are mainly sandy loam (<40 cm) mixed with a high gravel and stone content. The SF soils do not contain a clay layer and rests directly on the sandstone parent material. Gravel and stone content removal generally accompanies the transformation of SF to AF so as to improve crop drainage. Meteorological data were acquired from 2009 to 2011 with SensorScope (Ss) wireless environmental monitoring stations and EC towers distributed over SF and the adjacent AF (Figure 1). The Ss measures mean wind speed and direction at 2 m, air temperature, and relative humidity at 1.5 m, precipitation intensity, incoming solar radiation at 2 m, skin temperature with radiometer positioned at 1 m, and soil moisture at different depths (=0.05, 0.1, 0.2, 0.4 m). All variables were sampled or summed every 5 min and averaged or summed every 30 min. Three Ss stations were situated within the SF and six Ss stations were distributed within the AF to capture some of the spatial and temporal variability at each site, especially precipitation. The EC station included a three-dimensional sonic anemometer (CSAT3, Campbell Scientific, Logan UT) and an infrared gas analyzer (Licor7500, Licor, Lincoln, NE) situated at 2 m above the ground surface along with a net radiometer (Kipp and Zonen, Delft, The Netherlands). The sampling

frequency was 20 Hz and the averaging period was 30 min for all EC variables; postprocessing utilized the planar fit technique [*Pall et al*., 2007] to minimize errors caused by the sonic anemometer tilt.

3. Results

To address the study objectives, the results are structured as follows. An analysis delineating the differences in precipitation between AF and SF is first presented. Next, the crossing properties between modeled lifting condensation level (using Ss) and modeled convectively grown boundary layer height (forced with the eddy covariance sensible heat flux measurements) are explored. The fractional differences in measured daytime rainfall amounts across the two sites agree with the computed differences in crossing statistics. It is shown next that deviations in crossing statistics between AF and SF are mostly attributed to differences in boundary layer dynamics that are sensitive to land cover type (mainly sensible heat) instead of lifting condensation level. A plausibility argument that differences in rainfall amounts between AF and SF is convectively driven instead of topographically induced is also presented given that the SF site is at a higher elevation than the AF (see Figure 1).

Figure 2 shows a comparison between measured cumulative daytime precipitation from all the stations at the AF and SF sites for all 3 years. Daytime is defined as the time when the sensible heat flux switched signs from negative to positive (sunrise) and from positive to negative (sunset), which almost corresponded to 6 A.M.−6 P.M. ($\pm$ 15 min). Such cumulative precipitation comparison, known as the double mass analysis [*Kohler*, 1949], is conventionally used to assess the consistency among rainfall gages. The nighttime precipitation is not included here as the focus is on convective rainfall. Based on the measurements, daytime rain explains some 65% of the total rainfall. Figure 2 demonstrates that the rain gage network in the SF recorded a 10–30% higher daytime precipitation when compared to the AF site both for years with droughts and for wet years. These site differences are statistically significant and not connected to errors or biases in tipping bucket gage measurements because the double-mass analysis used Figure 2 shows all gages at SF recorded higher rainfall than any of the gages at AF. To place these precipitation differences in a regional context, it is noted that the measured differences in annual precipitation between AF and SF are larger than the temporal standard deviation in the 100 year annual precipitation fluctuations reported for the entire southwest Sahel [*Mahé and Paturel*, 2009] from 1896 to 2006 (shown in Figure 2) and exceeds all climatic change projections (in 2100) reported for the Sahel region [*Hulme et al*., 2001] in a doubled atmospheric CO_2 concentration scenario. It can be surmised from the data in Figure 2 that replacing SF with AF may lead to reduction in daytime rainfall that cannot be ignored. What is not evident from Figure 2 is the precise pathway leading to such reduction.

It has been known for some time that land cover impacts convective rainfall occurrence and amounts at local and continental scales [*Kanae et al*., 2001; *Pielke*, 2001; *Findell and Eltahir*, 2003; *Koster et al*., 2004, 2006; *Santanello et al*., 2007; *Pielke et al*., 2007; *Juang et al*., 2007b; *Mölg et al*., 2012; *Bonetti et al*., 2015]. Describing the initiation and amounts of convective rainfall remains a daunting scientific task [*Muller et al*., 2009; *Tao et al*., 2012], but its "predisposition" can be distilled to a minimum necessary crossing of the mixed layer height (h) and lifting condensation level (H_{LCL}). This condition is necessary to ensure condensation and subsequent cloud formation but cannot be sufficient to ensure rainfall occurrences as available energy for parcels to attain the level of free convection ($>h$) and cloud condensation nuclei (CCN) must be considered at this stage. It is for this reason that the h-H_{LCL} crossing is labeled as predisposition instead of triggering for convective rainfall. The mixed layer is a region where the air column thickness ($=h$) expands due to heating from the land surface and heating caused by entrained air originating from the free troposphere. The time evolution of h depends on the diurnal history of surface sensible heat flux, while the evolution of H_{LCL} primarily depends on the diurnal variations in mean air temperature and mean air relative humidity [*Juang et al*., 2007a, 2007b; *Siqueira et al*., 2009; *De Arellano et al*., 2012]. Seasonal variation in mean air temperature and relative humidity along with other synoptic scale disturbances do influence precipitation. These effects are indirectly accounted for through the calculation of H_{LCL}. Seasonal and synoptic-scale variations govern lower atmospheric air temperature and relative humidity variations that are measured by the SensorScope stations and used to compute the diurnal variation of H_{LCL} as earlier noted. The minimum necessary condition of h crossing H_{LCL} is employed here so as to assess whether replacing SF with AF explains the reductions in convective rainfall patterns using southeastern Burkina Faso as a prototypical system. It is

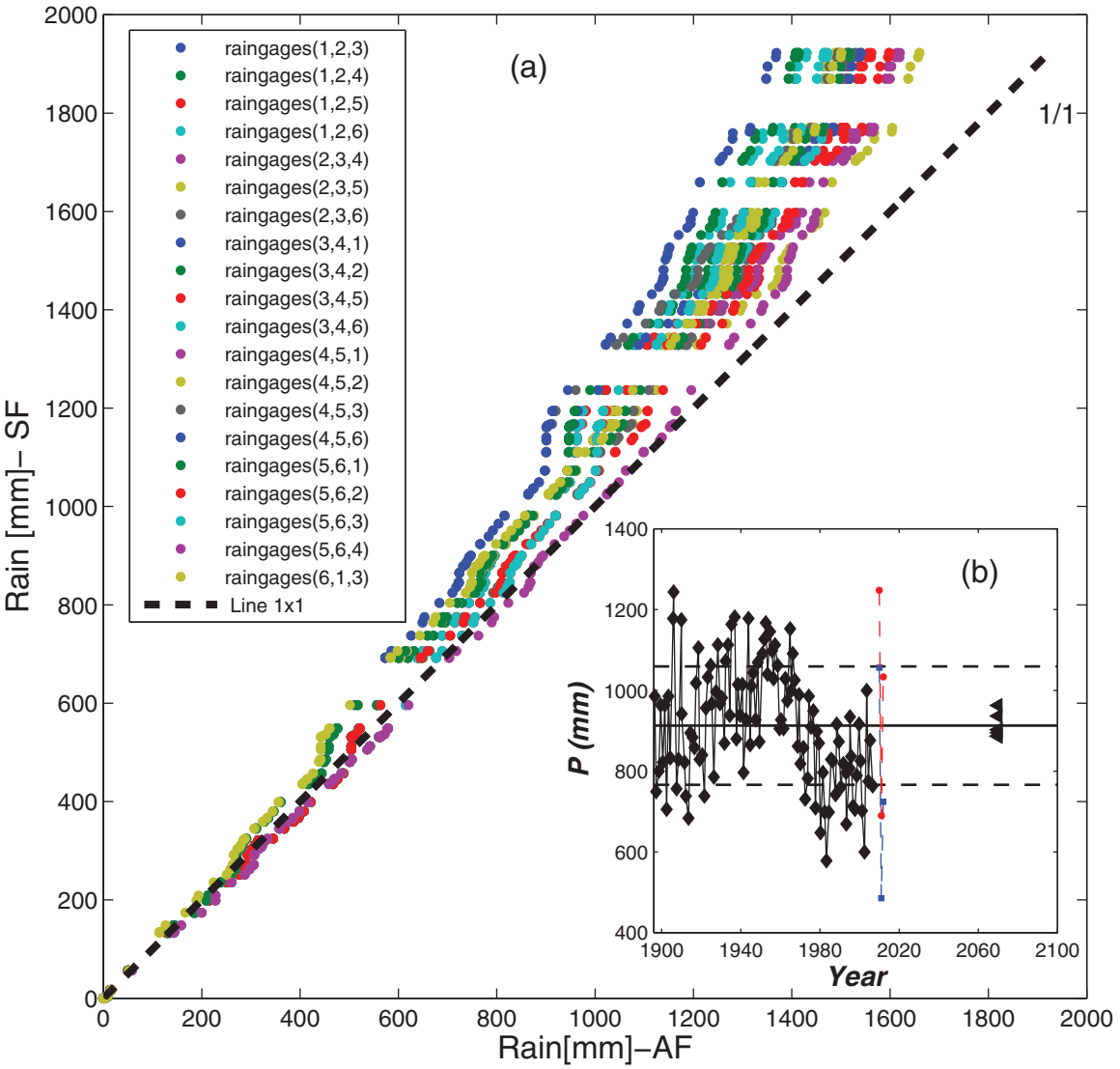

Figure 2. (a) Comparison of daytime cumulative precipitation between three rain gauges of the savannah forest (SF) and all combinations (i,j,k)of the rain six gauges over the agricultural field (AF). (b) Annual rainfall variability for past and future projections. Diamonds are from a long-term record for the Southwest Sahel region (1886–2006), triangles are climate model projections for the Sahel region in a doubled atmospheric CO_2 scenario and for different climate models. The annual rainfall at SF (rectangle) and AF (circle) for the study sites and the experimental period are also featured.

demonstrated that upon replacing SF by AF at spatial scales much larger than h lowers h but does not appreciably impact H_{LCL} during the wet season. The suppression of sensible heat flux resulting from an SF to AF conversion leads to a reduction in the crossing probability of h and H_{LCL}. It is further shown that the reason why H_{LCL} is not appreciably impacted by land cover is that the water vapor source within the mixed layer is not originating from the land surface during the wet season. However, sensible heat flux driving h dynamics are differents. Measured differences in surface water vapor fluxes are not large as these surface water vapor fluxes do not deviate appreciably from their near-wet surface evaporation values at both sites (determined by a Priestley-Taylor-type formulation). A one-dimensional slab model [*Juang et al.*, 2007a, 2007b] coupled to an encroachment closure hypothesis linking h to measured sensible heat flux time series is employed at the two sites. The slab model neglects advection and subsidence [*Stull*, 1988; *Garcia et al.*, 2002; *Juang et al.*, 2007a, 2007b] but was shown to be effective at reproducing mixed-layer heights [*Pino et al.*, 2006; *Gentine et al.*, 2013]. The H_{LCL} was estimated from diurnal variation of measured mean air temperature, air humidity, and atmospheric pressure.

Figure 3shows atypical case of modeled h and H_{LCL} evolution during the day using measured sensible heat flux (H) time series, and the mean air temperature and relative humidity as input (see Appendix A) at both

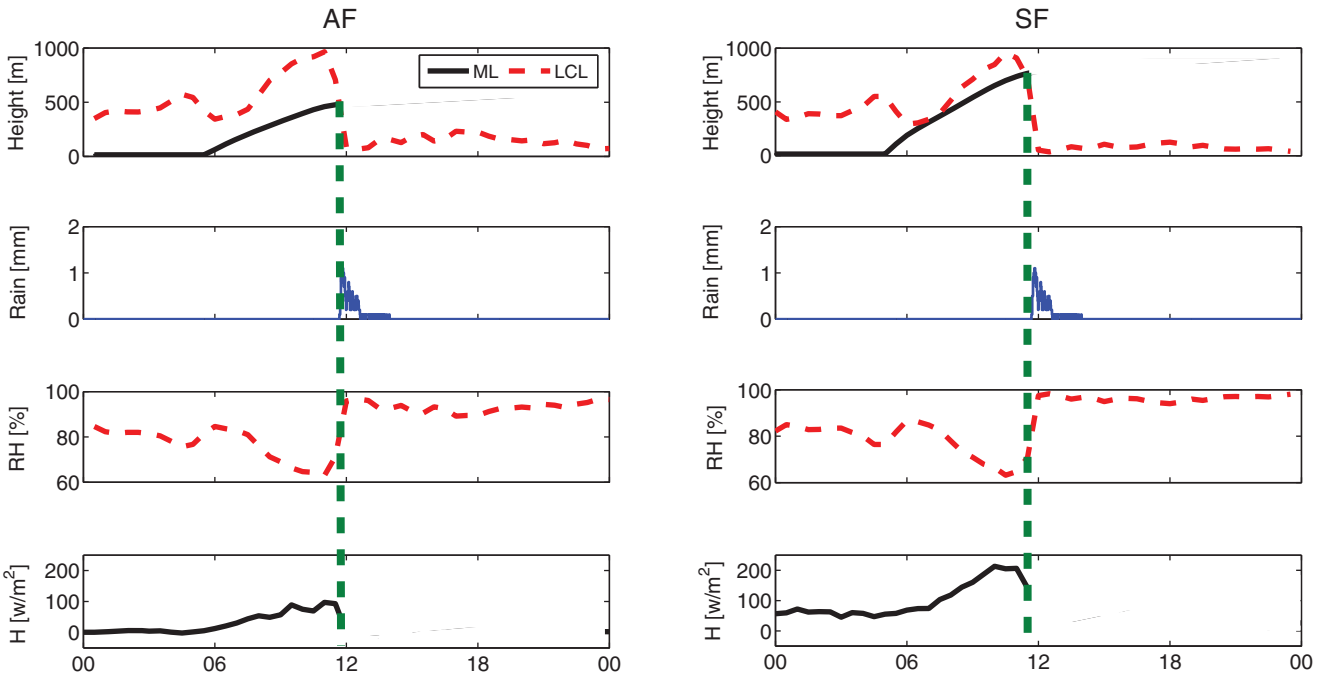

Figure 3. Modeled mixed layer height h and lifting condensation level H_{LCL} as a function of time of day along with the main drivers responsible for their variation for AF (left) and SF (right) for 2 July 2010. Note the rainfall occurrence over AF (left) and SF (right) following the modeled h- H_{LCL} crossing. The measured sensible heat flux (H) is higher over SF resulting in larger h but the H_{LCL} remain comparable at the two sites.

AF and SF. Shortly after the modeled h intersects H_{LCL}, rainfall is measured by the tipping bucket gage network at both sites. When air parcels are lifted by the thermals controlling h and reach H_{LCL}, condensation proceeds in regions of negatively buoyant overshoots within these thermals. If the overshoot kinetic energy is sufficiently large, additional lifting of condensing air parcels occurs. Latent heat is released from the lifted air parcels and their potential temperature becomes sufficiently warmer than their surrounding thereby allowing them to become positively buoyant and propelling further ascent. This height defines the so-called level of free convection, which is higher than H_{LCL}. The parcels may continue to rise buoyantly until they eventually become cooler than their surrounding atmosphere at which point the so-called limit of convective rise is reached. Any residual inertia in the parcels might propel them to further rise eventually terminating their ascent at the cloud top [*Stull*, 1988; *Emanuel et al.*, 1994]. Once clouds develop, condensation nuclei are required to allow for rapid growth in water droplets. If these droplets reach sufficient size to precipitate and repenetrate the unsaturated air below the cloud base without completely reevaporating before reaching the ground surface, rainfall at the surface is detected. After the $h - H_{LCL}$ crossing, this entire process can be completed on time scales ranging from minutes to few hours. At SF and AF sites, when rainfall was recorded by the tipping bucket gage network, the fraction of events occurring within 3 h after the h and H_{LCL} crossing exceeded 96%. There were no events in our analysis in which rainfall occurred without being preceded by an h - H_{LCL} crossing. Having demonstrated that the crossing of h and H_{LCL} appears to be a plausible necessary condition for cloud formation and rainfall predisposition, it is now used to diagnose whether land cover explains the measured rainfall differences between AF and SF reported in Figure 2.The computed H_{LCL} using measured mean air temperature and mean relative humidity are similar at both sites (Figure 4). Moreover, similarity in computed H_{LCL} suggests that the external water vapor source entrained or advected into the boundary layer dictates the mean air relative humidity within h at both sites, not the water vapor sources from the land surface. In fact, the latent heat (LE) fluxes measured at both sites are comparable and do not appreciably deviate from their wet surface value given by the Priestley-Taylor (PT) equation [*Priestley and Taylor*, 1972] with a PT coefficient of 1.26. It can be surmised from Figure 4 that land cover differences do not appreciably impact H_{LCL} in the wet season here, presumably due to the weak land surface controls on the water vapor concentration within the mixed layer column. However, the measured sensible heat flux at SF is some 1.4 times larger than its counterpart at AF (Figure 4). Differences in sensible heat fluxes but similarity in latent heat fluxes suggests that either net radiation is reduced at the SF site or

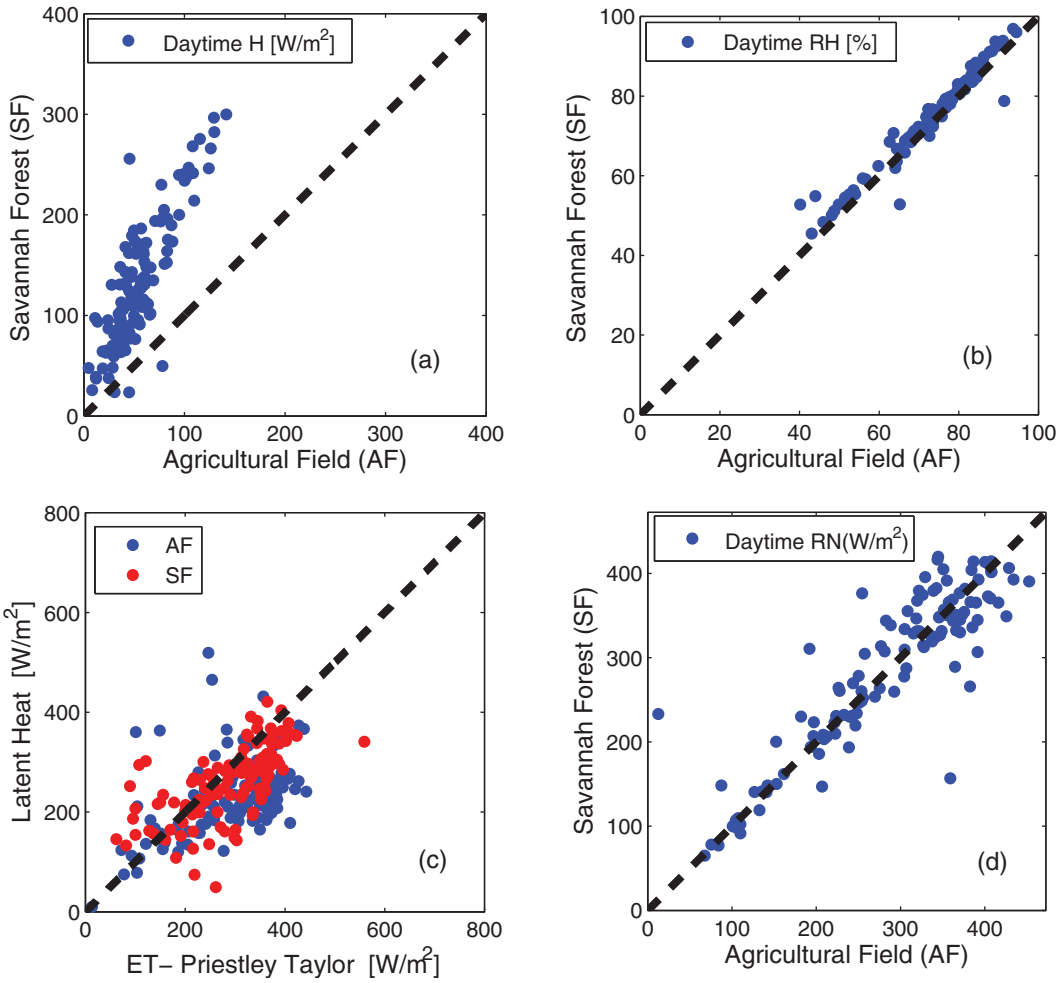

Figure 4. Comparison between measured (a) sensible heat flux (H), (b) daytime relative humidity (RH), (c) Latent Heat flux (LE) versus Priestley Taylor estimates, and (d) net radiation (RN). All variables were computed or measured simultaneously at AF and SF.

soil heat fluxes must be smaller at SF when compared to AF. Figure 4 suggests that net radiation differences between AF and SF cannot explain the 1.4 increase in measured sensible heat flux. In fact, the differences in net radiation between AF and SF were not significantly different from each other. Given the constraints imposed by the energy balance, the results in Figure 4 imply that differences in sensible heat flux are likely to be due to differences in soil heat fluxes (and possible canopy storage in SF) across the two sites. Soil heat flux measurements were not conducted here primarily because of the heterogeneous rock-soil vegetation cover environment at the remote SF site. Hence, we can only offer speculations as to why large soil heat flux differences between sites exist. Several key factors influencing soil heat flux vary between the SF and AF. The forested region soils are characteristically coarser textured, and therefore better drained than those of the agricultural areas. The SF soils also have much higher proportion of rock fragments at the surface. Rocks and rock fragments are manually removed from the agricultural fields consistent with agricultural practices. While the thermal conductivity of rocks is expected to be larger than that of bulk soil, the fact that the soil is well drained in SF creates large air pockets between the rock (and its fragments) and the adjacent soil particles thereby reducing the overall thermal conductivity (and soil heat flux) of the rock-soil system. Here, the lack of soil moisture means that air gaps act as effective "insulators" to heat conduction in SF. Conversely, wetter soil moisture states in AF allow water in soil pores to act as "thermal bridges" between individual solid grain particles thereby enhancing the overall thermal conductivity of the soil-water system. Another factor impacting the differences in soil heat flux is vegetation cover. As evident from the photographs in the map figure, the AF is nearly bare during the early phases of the growing season while the soil surface in SF is reasonably covered by vegetation. Maximum leaf area index (LAI) was not

measured at the two sites; however, MODIS based maximum Net Difference Vegetation Index (NDVI) at AF was 25–30% smaller than its NDVI counterpart in SF when using MODIS pixels closest to the EC towers. While conversion from NDVI to LAI cannot be readily undertaken and is fraught with uncertainties, a lower NDVI at AF is suggestive that vegetation cover is likely to be less when compared to SF even when AF is at its maximum LAI. To summarize, while the precise cause of enhanced soil heat in AF versus SF may be debated and the aforementioned mechanism is purely speculative, the fact remains that measured daytime sensible heat is some 1.4 times larger in SF versus AF, and it is this difference that is most pertinent to convective rainfall predisposition.

Model calculations show that the excess sensible heat at SF leads to some 30% more frequent h - H_{LCL} crossing, which is commensurate with the extra daytime rainfall recorded at SF when compared to AF. Moreover, the higher sensible heat flux at SF is consistent with higher probability of rainfall occurrence or yield (~37% at SF versus 23% at AF) following the h-H_{LCL} crossing. Higher sensible heat flux at SF ensures that uplifted air parcels within thermal plumes have sufficient kinetic energy to become positively buoyant and be propelled to the level of free convection thereby yielding more rainfall.

It is conceivable that some of the topographic variations (see Figure 1) between SF and AF may explain the rainfall differences. This elevation difference is included in surface pressure calculations needed in H_{LCL}; however, the possibility of orographic lifting effects on h was not directly considered. Indirectly, an analysis on the histogram of Ss measured mean wind speeds 2 h prior to the measured rainfall occurrences was conducted. The histogram analysis suggests that these wind speeds are reasonably small (mode under 0.5 m s^{-1} in SF and in AF and more than 95% of events are below 2 m s^{-1} in SF and SF). Likewise, the histogram of EC based measured friction velocities at AF and SF 2 h prior to measured rainfall has a mode of 0.1 m s^{-1} and rarely exceeded 0.3 m s^{-1}. This analysis is suggestive of (i) low mechanical production of turbulent kinetic energy driving the dynamics of h and (ii) lack of any large scale mean pressure gradient flow often associated with advection. Also, the concomitant wind direction did not exhibit any coherent spatial pattern among the SensorScope stations in SF and AF for the same periods. For SF, the most likely wind direction does not coincide with the maximum topographic gradient along the hill (data not shown). These two findings provide some (anecdotal) evidence that orographic effects impacting h or advection of moisture from one region to the other (e.g., SF to AF) is less likely. They are also consistent with the working assumption that convective processes are the dominant ones (low wind speed, variable wind direction) impacting the dynamics of h and its crossing with H_{LCL}.

To further explore this work assumption, scaling laws of the daytime rainfall intensity probability density function (*pdf*) are compared to expectations from sites dominated by summertime convective storm systems. If the daytime rainfall intensity scaling laws at the two sites appear to be commensurate with sites dominated by convective systems, then it is likely that the rainfall at both sites here originated from convective instead of orographic lifting. Figure 5 shows that the *pdf* of measured daytime rainfall intensity i at both sites exhibits nearly identical power-law regimes. This finding hints that the rainfall generation mechanism at the two sites must be similar; however, it does not disprove the orographic uplifting possibility. When a power law ($pdf(i)=Ci^{\alpha}$) is fitted to the rainfall data at AF and SF, an exponent $\alpha=-3/2$ emerges for the range of i covered by the measurements here. This α is comparable to α reported from an 8 year record at a site dominated by summertime convective rainfall (near Durham, North Carolina, USA), also shown in Figure 5. This similarity in α across SF and AF (and other convectively dominated rainfall sites) could be used to argue against possible orographic effects as being the culprit explaining the differences in mean rainfall due to elevation differences between the AF and SF sites.

With regards to using these intensity power laws in Figure 5 for extrapolating extremes beyond the limits of the measurements, a few cautionary comments must be added. First, it did not escape our attention that when assuming a power-law intensity *pdf* $i \in [i_{min}, +\infty]$, the ensemble mean rainfall intensity $<i>$ normalized by the minimum intensity i_{min} detected by the tipping bucket gage (=0.2 mm) and given by $<i>/i_{min} = (-\alpha-1)/(-\alpha-2)$ is statistically divergent for $\alpha=-3/2$. In practice, this mathematical divergence is unlikely to persist because the maximum intensity is bounded by finite precipitable water in the clouds. That is, physical limits on maximum precipitable water ensures that the "fat-tailed" power law in Figure 5 is "censored" thereby eliminating the divergence issue in the fitted $pdf(i)$. As to why α is close to $-3/2$ for a broad range of intensities is an interesting question recently examined in the context of convective rainfall and intermittency models [*Rigby and Porporato*, 2010]. It has been conjectured that some dynamical models

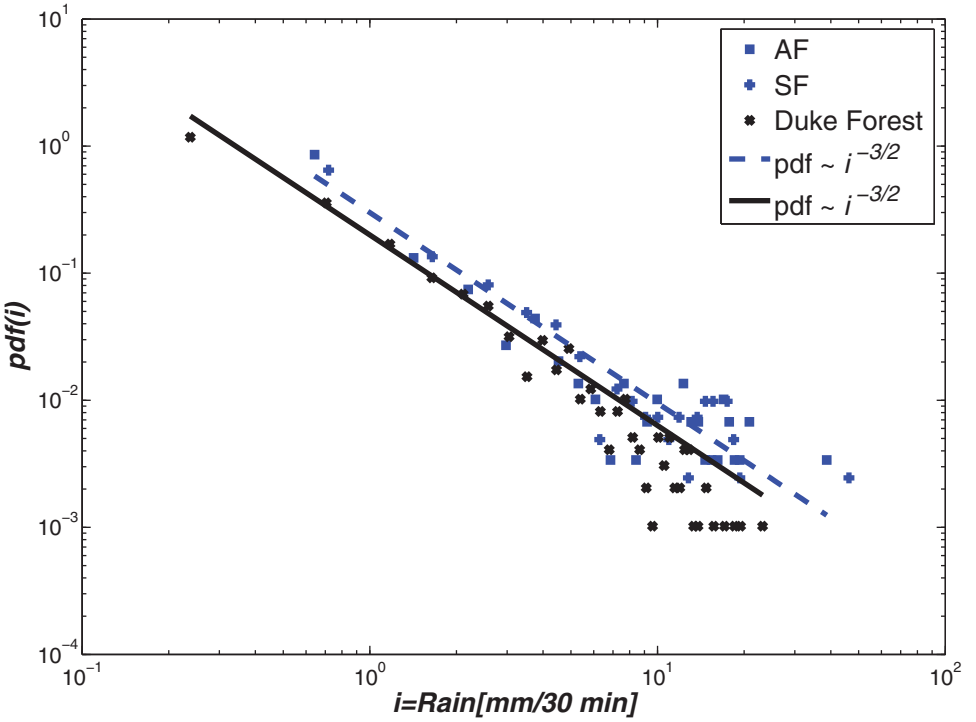

Figure 5. Measured rainfall intensity probability density function (*pdf*) at AF and SF. Comparison between these measurements and an 8 year record collected during the summer time in the Southeastern United States (Duke Forest, Durham, NC) dominated by convective storms is shown. Note that both *pdf* records exhibit an approximate power-law scaling with an exponent of $-3/2$ suggesting that convective rainfall activity, not orography, dominates rainfall amounts.

of intermittency are similar to convective rainfall, including the so-called Pomeau-Manneville Type-III intermittency. Such intermittency manifests a behavior intermediate between quasiperiodic and pure randomness known as "sporadic" randomness. Using the record from the Duke Forest (as used in Figure 5), it was shown that the probability distribution of laminar or quiescent phase durations and the spectrum of rainfall intensity time series are broadly consistent with a Pomeau-Manneville Type-III intermittency. However, the power-law exponent of the $pdf(i)$ as predicted bya Pomeau-Manneville Type-III intermittency is closer to -2 whereas the measured $pdf(i)$ in Figure 5 is closer to $-3/2$, an intermediate between on-off type intermittency and Type-III intermittency. This intermittency behavior may be plausible here as the dynamics of convective cells are quasideterministic in their growth and build up during the storm but are subsequently disrupted by the occurrence of rainfall (when the CCN microphysics allows it).

To summarize, similarity in measured α exponents across AF and SF suggests that the rainfall initiation mechanism must be similar (i.e., either both convective or both orographic). Furthermore, the fact that $\alpha = -3/2$ at both sites and agree with a reported $\alpha = -3/2$ at a site dominated by summertime convective rainfall suggests that the rainfall initiation mechanism at AF and SF is not only similar but originates from convective instead of orographic effects.

All these results support the main conjecture that daily mean rainfall at SF is larger than AF due to the more frequent crossings between ML and LCL associated with elevated sensible heat flux at SF. The impacts of orography at this site appear to be insufficient to induce the differences that are observed here.

4. Discussion and Conclusions

In water-limited areas, rainfall is the most crucial climatic parameter impacting directly the productivity and quality of life [*Intergovernmental Panel on Climate Change*, 2002; *Pall et al.*, 2007]. Given the United Nations Millennium Development Goals that argue for green economic policies in Africa, understanding land cover changes and its impact on the spatial and temporal rainfall dynamics is now urgent. The effect of land cover change on precipitation pattern at larger scales has been reported in several studies [*Pielke and Avissar*, 1990;

Avissar and Schmidt, 1998; *Chase et al*., 2001; *Mölg et al*., 2012; *Pall et al*., 2007; *Pielke et al*., 2007; *Douglas et al*., 2009]. Using novel data and simplified model calculations from a data-poor region experiencing rapid land-cover change, the data-model analysis here suggests a potential impact of such land cover change on the precipitation pattern at local scales of several kilometers. Land use signature on the convective rainfall mechanism is highlighted by water vapor controlled by regional forcing while the sensible heat flux is locally controlled with a 40% difference from AF to SF. Land use change does not only include the vegetation cover but also the soil properties (e.g., plowing and the removing of stones) and subsequent consequences for water movement, drainage, and local energy balance. The local sensible heat flux enhances the likelihood of ML and LCL crossing as demonstrated here. Future research will focus on occurrences and the partitioning of extreme events at small scales and their hydrologic consequences in arid and semiarid areas. Further analysis on the coupled soil heat and moisture flow at SF (and AF) in three dimensions is clearly warranted to constrain the causes of the enhanced sensible heat flux over SF when compared to AF.

Appendix A

The ML height h was determined from a mixed-layer slab model and by adopting the encroachment closure for potential temperature T_p [*Stull*, 1976, 1994; *Garcia et al*., 2002] and by ignoring the contribution of heat sources and sinks within the ML to yield,

$$\frac{dh}{dt} = \frac{H_s - H_t}{\rho C_p \gamma},$$

where H_s is the measured sensible heat flux at the surface, H_t is the entrainment flux modeled as $H_t = -\beta H_s$, ρ is the mean air density, C_p is the specific heat capacity of dry air at constant pressure, and $\gamma = g/C_p$ is the lapse rate approximated by its dry adiabatic value, $g = 9.8$ m s^{-2} is the gravitational acceleration, and β is a constant that varies between 0.2 and 0.4, with a mean of 0.3 [*Kim and Entekhabi*, 1998] selected here. To solve this differential equation, an initial condition of $h(0) = 15$ m was set when H_s switches from negative (night) to positive (day). For the LCL, denoted by H_{LCL},

$$H_{LCL} = \frac{RT}{Mg} log\left(\frac{P_s}{P_{LCL}}\right),$$

where R is the Universal gas constant (=8.314 J mol^{-1} K), M is the molecular weight of dry air (~29 g mol^{-1}), T (K) is the mean air temperature, P_s is the local surface atmospheric pressure (kPa), and P_{LCL} (kPa) can be calculated from the hydrostatic approximation,

$$\frac{P_s}{P_{LCL}} = \left(\frac{T_{LCL}}{T}\right)^{3.5},$$

where T_{LCL} is the saturation temperature at the H_{LCL} given by *Stull* [1994]

$$T_{LCL} = 55 + \frac{2840}{3.5 \ln(T) - ln\left(\frac{P_s r}{0.622 + r} - 7.108\right)},$$

where r is the near-surface water vapor mixing ratio derived from the measured air relative humidity. Here, the minor elevation differences between AF and SF is accounted for in P_s.

Acknowledgments
We are grateful to the peer reviewers who helped improve the manuscript. We appreciate funding and support from the Swiss development agency, the Swiss NSF, The NCCR (Mobile Information Communication Systems), and the NSERC Discovery grant to M.B.P. We would also like to acknowledge the assistance and support of the village of Tambarga that was essential in the field work. G.K. acknowledges support from the National Science Foundation (NSF-AGS-1102227 and NSF-EAR-1344703), and the U.S Department of Energy (DOE) through the Office of Biological and Environmental Research (BER) Terrestrial Carbon Processes (TCP) program (DE-SC0006967 and DE-SC0011461). If the manuscript is accepted for publication, the data reported here will be archived at CDIAC that houses the FLUXNET database (http://fluxnet.ornl.gov/obtain-data).

References

Avissar, R., and T. Schmidt (1998), An evaluation of the scale at which ground-surface heat flux patchiness affects the convective boundary layer using large-eddy simulations, *J. Atmos. Sci.*, *55*(16), 2666–2689, doi:10.1175/15200469.

Bagayoko, F., S. Yonkeu, J. Elbers, and N. van de Giesen (2007), Energy partitioning over the West African savanna: Multi-year evaporation and surface conductance measurements in Eastern Burkina Faso, *J. Hydrol.*, *334*(3-4), 545–559.

Bonetti, S., G. Manoli, J. C. Domec, M. Putti, M. Marani, and G. G. Katul (2015), The influence of water table depth and the free atmospheric state on convective rainfall predisposition, *Water Resour. Res.*, *51*, 2283–2297, doi:10.1002/2014WR016431.

Ceperley, N. C., A. Repetti, and M. B. Parlange (2012), Application of soil moisture model to Marula (*Sclerocarya birrea*): Millet (*Pennisetum glaucum*) agroforestry system in Burkina Faso, in *Technologies and Innovations for Development*, edited by J.-C. Bolay et al., pp. 211–229, Springer, Paris.

Chase, T. N., R. A. Pielke, T. G. F. Kittel, M. Zhao, A. J. Pitman, S. W. Running, and R. R. Nemani (2001), Relative climatic effects of landcover change and elevated carbon dioxide combined with aerosols: A comparison of model results and observations, *J. Geophys. Res.*, *106*(D23), 31,685–31,691, doi:10.1029/2000JD000129.

De Arellano, J. V.-G., C. C. van Heerwaarden, and J. Lelieveld (2012), Modelled suppression of boundary-layer clouds by plants in a CO2-rich atmosphere, *Nat. Geosci.*, *5*(10), 701–704, doi:10.1038/ngeo1554.

Douglas, E. M., A. Beltrán-Przekurat, D. Niyogi, R. A. Pielke, and C. J. Vörösmarty (2009), The impact of agricultural intensification and irrigation on and–atmosphere interactions and Indian monsoon precipitation: A mesoscale modeling perspective, *Global Planet. Change*, *67*(1–2), 117–128, doi:10.1016/j.gloplacha.2008.12.007.

Emanuel, K. A., J. D. Neelin, and C. S. Bretherton (1994), On large-scale circulations in convecting atmospheres, *Q. J. R. Meteorol. Soc.*, *120*(519), 1111–1143, doi:10.1002/qj.49712051902.

Findell, K. L., and E. A. B. Eltahir (2003), Atmospheric controls on soil moisture-boundary layer interactions. Part I: Framework development, *J. Hydrometeorol.*, *4*(3), 552–569, doi:10.1175/1525-7541.

Garcia, J. A., M. L. Cancillo, and J. L. Cano (2002), A case study of the morning evolution of the convective boundary layer depth, *J. Appl. Meteorol.*, *41*(10), 1053–1059.

Gentine, P., C. R. Ferguson, and A. A. M. Holtslag (2013), Diagnosing evaporative fraction over land from boundary-layer clouds, *J. Geophys. Res. Atmos.*, *118*, 8185–8196, doi:10.1002/jgrd.50416.

Hulme, M., R. Doherty, T. Ngara, M. New, and D. Lister (2001), African climate change: 1900–2100, *Clim. Res.*, *17*(2), 145–168, doi:10.3354/cr017145.

Intergovernmental Panel on Climate Change (2002), *IPCC Workshop on Changes in Extreme Weather and Climate Events*, 107 pp., Beijing, China.

Juang, J. Y. I. H., G. G. Katul, A. Porporato, P. C. Stoy, M. S. Siqueira, M. Detto, H. S. Kim, and R. Oren (2007a), Eco-hydrological controls on summertime convective rainfall triggers, *Global Change Biol.*, *13*(4), 887–896.

Juang, J. Y., A. Porporato, P. C. Stoy, M. S. Siqueira, A. C. Oishi, M. Detto, H. S. Kim, and G. G. Katul (2007b), Hydrologic and atmospheric controls on initiation of convective precipitation events, *Water Resour. Res.*, *43*, W03421, doi:10.1029/2006WR004954.

Kanae, S., T. Oki, and K. Musiake (2001), Impact of deforestation on regional precipitation over the Indochina Peninsula, *J. Hydrometeorol.*, *2*(1), 51–70, doi:10.1175/1525-7541(2001)002<0051:IODORP>2.0.CO;2.

Kim, C. P., and D. Entekhabi (1998), Feedbacks in the land-surface and mixed-layer energy budgets, *Boundary Layer Meteorol.*, *88*(1), 1–21, doi:10.1023/A:1001094008513.

Kohler, M. A. (1949), Double mass analysis for testing consistency of records and for making required adjustments, *Bull. Am. Meteorol. Soc.*, *30*, 188–189.

Koster, R. D., et al. (2004), Regions of strong coupling between soil moisture and precipitation, *Science*, *305*(5687), 1138–1140, doi:10.1126/science.1100217.

Koster, R. D., et al. (2006), GLACE: The global land–atmosphere coupling experiment. Part I: Overview, *J. Hydrometeorol.*, *7*(4), 590–610, doi:10.1175/JHM510.1.

Mahé, G., and J.-E. Paturel (2009), 1896–2006 Sahelian annual rainfall variability and runoff increase of Sahelian Rivers, *C. R. Geosci.*, *341*(7), 538–546, doi:10.1016/j.crte.2009.05.002.

Mande, T., N. C. Ceperley, S. V. Weijs, A. Repetti, and M. B. Parlange (2014), Toward a new approach for hydrological modeling: A tool for sustainable development in a Savanna Agro-System, in *Technologies for Sustainable Development*, edited by J.-C. Bolay, S. Hostettler, and E. Hazboun, pp. 85–98, Springer, Switzerland.

Mölg, T., M. Großhauser, A. Hemp, M. Hofer, and B. Marzeion (2012), Limited forcing of glacier loss through land-cover change on Kilimanjaro, *Nat. Clim. Change*, *2*(4), 254–258. doi:10.1038/nclimate1390.

Muller, C. J., L. E. Back, P. A. O'Gorman, and K. A. Emanuel (2009), A model for the relationship between tropical precipitation and column water vapor, *Geophys. Res. Lett.*, *36*, L16804, doi:10.1029/2009GL039667.

Nicholson, S. E. (2013), The west African Sahel: A review of recent studies on the rainfall regime and its interannual variability, *ISRN Meteorol.*, *2013*, 1–32. doi:10.1155/2013/453521.

Pall, P., M. R. Allen, and D. A. Stone (2007), Testing the Clausius–Clapeyron constraint on changes in extreme precipitation under CO2 warming, *Clim. Dyn.*, *28*(4), 351–363, doi:10.1007/s00382-006-0180-2.

Pielke, R. A. (2001), Influence of the spatial distribution of vegetation and soils on the prediction of cumulus Convective rainfall, *Rev. Geophys.*, *39*(2), 151–177, doi:10.1029/1999RG000072.

Pielke, R. A., and R. Avissar (1990), Influence of landscape structure on local and regional climate, *Landscape Ecol.*, *4*(2-3), 133–155, doi:10.1007/BF00132857.

Pielke, R. A., J. Adegoke, A. Beltrán-Przekurat, C. A. Hiemstra, J. Lin, U. S. Nair, and T. E. Nobis (2007), An overview of regional land-use and land-cover impacts on rainfall, *Tellus Ser. B*, *59*(3), 587–601, doi:10.1111/j.1600-0889.2007.00251.x.

Pino, D., J. Vilà-Guerau de Arellano, and S.-W. Kim (2006), Representing sheared convective boundary layer by zeroth- and first-order-jump mixed-layer models: Large-eddy simulation verification, *J. Appl. Meteorol. Climatol.*, *45*(9), 1224–1243, doi:10.1175/JAM2396.1.

Priestley, C. H. B., and R. J. Taylor (1972), On the assessment of surface heat flux and evaporation using large-scale parameters, *Mon. Weather Rev.*, *100*(2), 81–92, doi:10.1175/1520-0493(1972)100<0081:OTAOSH>2.3.CO;2.

Rigby, J. R., and A. Porporato (2010), Precipitation, dynamical intermittency, and sporadic randomness, *Adv. Water Resour.*, *33*(8), 923–932, doi:10.1016/j.advwatres.2010.04.008.

Santanello, J. A., M. A. Friedl, and M. B. Ek (2007), Convective planetary boundary layer interactions with the land surface at Diurnal time scales: Diagnostics and feedbacks, *J. Hydrometeorol.*, *8*(5), 1082–1097, doi:10.1175/JHM614.1.

Siqueira, M., G. G. Katul, and A. Porporato (2009), Soil moisture feedbacks on convection triggers: The role of soil–plant hydrodynamics, *J. Hydrometeorol.*, *10*(1), 96–112, doi:10.1175/2008JHM1027.1.

Stull, R. B. (1976), Mixed-layer depth model based on turbulent energetics, *J. Atmos. Sci.*, *33*(7), 1268–1278, doi:10.1175/1520-0469(1976)033<1268:MLDMBO>2.0.CO;2.

Stull, R. B. (1988), *An Introduction to Boundary Layer Meteorology*, Springer, N. Y.

Stull, R. B. (1994), A convective transport theory for surface fluxes, *J. Atmos. Sci.*, *51*(1), 3–22, doi:10.1175/1520-0469(1994)051<0003:ACTTFS>2.0.CO;2.

Tao, W.-K., J.-P. Chen, Z. Li, C. Wang, and C. Zhang (2012), Impact of aerosols on convective clouds and precipitation, *Rev. Geophys.*, *50*, RG2001, doi:10.1029/2011RG000369.

USGS (2013), *Land Cover Applications and Global Change: USGS Land Cover Applications*, U.S. Department of the Interior, U.S. Geological Survey. [Available at http://lca.usgs.gov/lca.]